Numerical Simulation of the Critical Scale of Oasis Maintenance and Development in the Arid Regions of Northwest China

GAO Yanhong* (高艳红), CHEN Yuchun (陈玉春), and LÜ Shihua (吕世华)

Cold and Arid Regions Environmental and Engineering Research Institute, Chinese Academy of Sciences, Lanzhou 730000

(Received 18 December 2002; revised 5 September 2003)

ABSTRACT

Oasis is a special geographic landscape among the vast desert/Gobi in Northwest China (NWC). The surface sensitive heat flux and latent heat flux at Zhangye Oasis during 1 to 11 August 1991 are simulated using the NCAR nonhydrostatic mesoscale model MM5 Version 3. The horizontal grid resolution is set as 1km. By comparing the simulation results with HEIFE observations, it is proved that the model can be used to simulate the surface energy and water mass exchange of arid and semiarid regions in NWC. Based on the above results, the influence of different oasis scales on the local atmospheric field near the ground surface, and the critical scale of oasis maintenance, in NWC are studied dynamically. The following conclusion is obtained: the local thermal circulation between the oasis and the desert/Gobi is formed in the oasis downstream if the oasis scale is larger than 4 km. This local thermal circulation between the oasis and the desert adjacent to the oasis helps to conserve water vapor over the oasis. At the same time, it transfers the abundant water vapor from the oasis into the desert/Gobi near to the oasis to supply relatively plentiful water vapor for desert crops to grow on the fringe of the oasis. So, it is advantageous for oasis extension. However, if the scale of the oasis is smaller than 4 km, it is not easy for the local thermal circulation between the oasis and the desert/Gobi to take shape. This study provides a new standpoint for oasis maintenance and development.

Key words: MM5, oasis, desert/Gobi, critical scale, local thermal circulation

1. Introduction

1.1 *Background*

The oasis comprises only 5% of the area in arid/semiarid regions of Northwest China (NWC), but it plays an important role in feeding over 95% of the population. The oasis is a special ecosystem opposing the dry environment in arid regions (Zhang and Hu, 2001). The area of each oasis is different. Some of them are large and some small. Their location and surrounding natural environment are dissimilar. Their own characteristics are disparate also. In other words, the natural and unnatural conditions are not same in different oases. The laws of development and evolution of every oasis differ very much. So, no doubt, each oasis performs its own processes of formation and evolution history.

There is hardly any natural rainfall due to the oasis existing under the arid background. Supplying sufficient water becomes the basic necessary condition for the oasis' existence and extension. The scale of the oasis plays an important role in its own maintenance keeping and development process.

During summer, a scorching and extreme arid environment forms and lasts for a long time. The Gobi, or the desert, is under the condition of cloudless or partly cloudy weather in the arid region in Northwest China (NWC). A strong turbulence is developed over the Gobi or the desert in the daytime, because the stratification is extremely unstable. But at the same time, the development of turbulence causes a stable inverse stratification over the oasis cold island. The oasis forms a stable cool and humid microclimate. The cold island is a stable cold-air parcel having stable stratification inside, and it has a clear boundary and it is difficult for the mass to exchange between the inside and the outside. A series of phenomena illustrates that the cold island has stable conservation. It is conducive to

*E-mail: gaoyh@ns.lzb.ac.cn

vegetative growth, because the cool and moist environment, and weaker turbulence control vegetation transpiration and soil evaporation, and the cool and moist environment helps also to preserve both the limited water resources in NWC and is helpful for vegetation growth in the arid regions (Su et al., 1987b). On the other hand, the oasis cold island can also exchange energy and mass with the surroundings through the turbulence, the advection of local circulation. The reciprocal action of the cold island and the surroundings diffuses cool humid air into the surroundings and improves the microclimate of the oasis fringes (Zhang and Hu, 2001). It is beneficial for oasis maintenance and development.

No doubt, the series of characteristics of the microclimate displayed by the "oasis effect" plays a very important role in oasis ecosystem maintenance and development. It is not only because the superior light and heat resources are beneficial for land ecology and crop growth, but also more importantly because the special microclimate characteristics of oasis can reduce the invalid water vapor loss, and sustain oasis self-maintenance by forming the virtuous mechanism of oasis ecosystem maintenance and development (Zhang and Hu, 2001). How could oases surrounded by the vast dry and hot desert exist for such a long time and not be engulfed by the desert/Gobi surrounding them? It is explained in meteorological theory (Hu, 1989; Hu and Wang, 1989). The research on the "oasis effect" in arid and semiarid regions is necessary. It is a study not only of theoretical significance but also of practical use.

1.2 *Introduction of related research*

The temperature, humidity, and wind speed were recorded at the Gansu Institute of Agricultural Science (IAS) located at the west of Zhangye City, Gansu Province, and at Nandatan located at the south of Zhangye City, from 18 June to 22 July 1984. The microclimate characteristics over the oasis in the Hexi region have been studied by observing the gradients of the meteorological elements. An oasis cold island effect was discovered (Su et al., 1987a; Su and Hu, 1988). That is to say that the oasis in Gobi or desert under the condition of cloudless or partly cloudy weather during summer in the Hexi region is a cold source in comparison with the surroundings, and thus the oasis cold island is formed. The oasis "cold island" affects the construction of the planetary boundary layer and makes it adjust and vary according to it. It is a special meteorological phenomenon within the planetary boundary layer. It was again discovered in the HEIHE River Field Experiment (HEIFE). Inverse sensitive heat flux in the daytime was discovered over oasis adjacent to desert also, namely the oasis effect in the daytime (Hu and Wang, 1989; Hu et al., 1994).

A two-dimensional model coupling the land-surface processes and the atmospheric planetary layer motion is developed, and the local climate resulting from an oasis surrounded by desert is simulated with the coupled model (Ji and Miao, 1994). Zhang and Sang simulated the atmospheric boundary layer over a surface of a desert-grassland area using a three-dimensional mesoscale numerical model combined with the Simple Biosphere model (SIB). The mesoscale flux was compared with the turbulent flux in order to confirm the importance of the mesoscale movement, which is usually ignored in the surface parameterization scheme in GCM models. The results indicated that the mesoscale flux, especially the heat flux, should not be ignored over the inhomogeneous underlying surface (Zhang and Sang, 2000). The Pielke model was coupled with a combined land surface process model, which included a simplified canopy model and a simplified desert soil model. The numerical simulations were carried out on a typical heterogeneous land surface with the oasis and desert, which is distributed in the HEIFE experiment area, using this coupled model (Niu et al., 1997). The local climate effect of the heterogeneous underlying surface was simulated using the mesoscale model MM5. The influence of different oasis distributions on regional climate was studied also. The ground energy budget and the influence on the characteristics of the boundary layer were analyzed. It provides some insights into the mechanisms for governing the desertification (Gao and Lu, 2001a, b).

Oasis exists on its own scale. Zhang and Yu (2001) modeled an oasis-induced atmospheric mesoscale flow using a two-dimensional mesoscale atmospheric numerical model taking account of the condition of a simple land surface process. The sensitivities of the atmospheric mesoscale flow to the oasis horizontal spatial scale, thermal and dynamical difference between oasis and near desert, large-scale horizontal wind speed, and large-scale surface sensitive heat flux were studied. It was found that the oasis-induced atmospheric mesoscale flow becomes strong with an increase of thermal and dynamic difference between the oasis and the near desert. And it becomes weak with the increase of large-scale horizontal wind speed and large scale surface sensible heat flux; but the intensity change of the mesoscale motion with the horizontal spatial scale of the oasis is not a monotonous function. The atmospheric mesoscale motion is the strongest when the horizontal spatial scale of the oasis reaches about 20 km and becomes weak when the oasis horizontal scale is less or larger. That means the best scale of the oasis is 20 km (Zhang and Yu, 2001).

The characteristics of the oasis-desert interaction were studied dynamically and thermodynamically based on a simplified dynamic model and the entropy budget equation, which describe the energy and moisture exchange between the oasis and the desert. The dependence of the oasis evaporation rate on the oasis scale is revealed. Negative entropy occurs when the oasis scale is less than about 6 km (Xue and Hu, 2001).

A two-dimensional and steady state numerical model of the planetary boundary layer was developed to analyze the structure of the "cold island" (Hu, 1987). It was also pointed out that there are many insufficiencies in the study of the oasis effect. Further theoretical and practical researches are therefore necessary. The critical scale of oasis maintenance and development is just one of these researches. The desert is in a condition of drought and intense heat and in unstable stratification under the summer sunshine. A small plot of grass or trees planted in the arid Gobi or the desert does not last long, because the small plot of oasis will be destroyed under the intense arid environment before the cold island effect is formed. That is to say that as long as the oasis in the arid Gobi or the desert is large enough to form a cold island, that will be a favorable microclimate for vegetation growth. Of course, this theory is helpful for planting grass and trees and developing agriculture in the arid region in Northwest China. The critical scale of oasis needs further study.

2. Brief description of the model

The model used here is the NCAR nonhydrostatic mesoscale model MM5. The horizontal grid is an Arakawa-Lamb B-staggering of the velocity variables with respect to the scalars. The vertical coordinate is terrain-following in that the lower grid levels follow the terrain until the upper surface is flat (Grell et al., 1995; Dudhia et al., 2001).

There are many physical process options for each parameterization scheme. The schemes are selected as the following: The cumulus parameterization (ICUPA) is the Grell scheme. The simple ice option is adapted as the explicit moisture scheme (IMPHYS). The radiation scheme (IFRAD) selected is the cloud-radiation scheme. The planetary boundary layer scheme (IBLTYS) is selected as the MRF PBL option; the modified Oregon State University Land-Surface Model (OSULSM) is chosen. Here is the brief description of the MRF PBL scheme and the OSU land surface model.

The NCAR nonhydrostatic atmospheric mesoscale model MM5 has been developed to version 3.5 in which the Oregon State University/NCEP Eta Land-Surface Model (LSM) was coupled (Chen and Dudhia, 2001). Chen et al. (1996) extended the Oregon State University LSM (OSULSM), which was originally developed by Pan and Mahrt (1987). This LSM is based on the coupling of the diurnally dependent Penman's potential evaporation approach of Mahrt and Ek (1984), the multiplayer soil model of Mahrt and Pan (1984), and the primitive canopy model of Pan and Mahrt (1987). It has been extended to include the modestly complex canopy resistance approach of Noihan and Planton (1989) and Jacquemin and Noihan (1990). It has one canopy layer and four soil layers. The thickness of each layer from the ground surface to the bottom is 0.1, 0.3, 0.6, and 1.0 m, respectively. The total soil depth is 2 m, with the root zone in the upper 1 m of soil. Thus, the lower 1 m soil layer acts like a reservoir with the gravity drainage at the bottom.

2.1 *PBL scheme and the surface layer parameterization*

The turbulent diffusion equation of diagnosed variations such as u, v, θ, and q in the MRF PBL is

$$\frac{\partial C}{\partial t} = \frac{\partial}{\partial z}\left[K_{\rm c}\left(\frac{\partial C}{\partial z} - \gamma_{\rm c}\right)\right] ,$$

in which $K_{\rm c}$ is the diffusion coefficient, $\gamma_{\rm c}$ is the adjusting factor of the temperature and humidity gradient in the mixing boundary layer, and it decides the calculation of the momentum, the heat capacity, and the water vapor fluxes with large scale diffusion. The momentum diffusion coefficient in the mixing boundary layer is expressed as

$$K_{zm} = k w_{\rm s} z \left(1 - \frac{z}{h}\right)^p .$$

Here, p is the index of the profile, k is the Kàrman constant, z is the height above the ground surface, h is the PBL height. In the free atmosphere layer, K theory is used. The vertical diffusion coefficients of momentum ($m : u, v$) and mass ($t : \theta, q$) are expressed as

$$K_{m,t} = l^2 f_{m,t}(Ri_{\rm g}) \left|\frac{\partial U}{\partial z}\right| ,$$

in which l is the mixing length $Ri_{\rm g}$ is the local gradient Richardson number, and $f_{m,t}(Ri_{\rm g})$ is the stability function being related to the vertical wind shear $\partial U/\partial z$.

The LSM is coupled to the MM5 model through the lowest atmospheric level, which is also referred to as the surface layer. A surface layer parameterization should provide the bulk exchange coefficients for the momentum, the heat, and the water vapor used to determine the flux of these quantities between the

land surface and the atmosphere. The surface layer parameterization base is its surface flux calculations based on similarity theory, using the stability function and the roughness length to determine the surface exchange coefficient for the heat and the moisture. This LSM scheme through the PBL is a component of the exchange coefficient together with the surface radiation forcing terms and the precipitation rate. The routine LSM with the PBL scheme calculate the boundary layer flux convergence, which contributes to the atmospheric temperature and moisture tendency, using the surface heat and moisture fluxes. Currently, the surface exchange coefficient for the heat and the moisture is formulated in MM5 as

$$C_{\rm h} = \frac{k^2 V_{\rm a}}{\left[\ln\left(\frac{z_{\rm a}}{z_{0m}}\right) - \psi_m\right]\left[\ln\left(\frac{z_{\rm a}}{z_{0t}}\right) - \psi_{\rm h}\right]} ,$$

in which the variable $z_{\rm a}$ is the height, take from the lowest computation level in the model, above ground; k is the Kàrman constant; and $V_{\rm a}$ is the wind speed at the lowest layer. The quantities z_{0m} and z_{0t} are the roughness lengths for the momentum and the heat, respectively. z_{0t} is defined as

$$z_{0t} = \frac{1}{\left(\frac{ku_*}{K_{\rm a}} + \frac{1}{z_l}\right)} ,$$

in which $K_{\rm a}$ is the molecular diffusivity u_* is the friction velocity, and z_l is a parameter (=0.01 m) related to molecular sublayer.

2.2 *LSM thermodynamics*

The surface skin temperature is determined by applying a single linearized surface energy budget equation representing the combined soil-vegetation surface, according to Mahrt and Ek (1984). The surface heat flux is controlled by the usual diffusion equation for soil temperature (T):

$$C\left(\Theta\right)\frac{\partial T}{\partial t} = \frac{\partial}{\partial z}\left[K_{\rm t}\left(\Theta\right)\frac{\partial T}{\partial z}\right] .$$

The volumetric heat capacity, C (J m^{-3} K^{-1}), and the thermal conductivity, $K_{\rm t}$ (W m^{-1} K^{-1}), are formulated as the functions of volumetric soil water content (Θ):

$$C = \Theta C_{\rm water} + (1-\Theta)C_{\rm soil} + (\Theta_{\rm s} - \Theta)C_{\rm air} ,$$

$$K_{\rm t}(\Theta) = \begin{cases} 420\exp[-(2.7+P_{\rm f})] , & P_{\rm f} \leqslant 5.1 \\ 0.1744 , & P_{\rm f} > 5.1 \end{cases}$$

and

$$P_{\rm f} = \log\left[\psi_{\rm s}\left(\Theta_{\rm s}/\Theta\right)^b\right] ,$$

The volumetric heat capacities are $C_{\rm water}$=4.2×10^6 J m^{-3} K^{-1}, $C_{\rm soil}$=1.26×10^6 J m^{-3} K^{-1}, and $C_{\rm air}$=1004 J m^{-3} K^{-1}. Here $\Theta_{\rm s}$ and $\psi_{\rm s}$ are maximum soil moisture (porosity) and saturated soil potential (suction), respectively, and both depend on the soil texture.

2.3 *LSM hydrology*

In the hydrology model, the prognostic equation for the volumetric soil moisture content Θ is

$$\frac{\partial\Theta}{\partial t} = \frac{\partial}{\partial z}\left(D\frac{\partial\Theta}{\partial z}\right) + \frac{\partial K}{\partial z} + F_\Theta ,$$

where both the soil water diffusivity D and the hydraulic conductivity K are functions of Θ. And F_Θ represents sources and sinks (i.e. precipitation, evaporation, and runoff) for soil water. The soil water diffusivity D is given by

$$D = K(\Theta)(\partial\psi/\partial\Theta) ,$$

where in ψ is the soil water tension function. K and ψ are computed by

$$K(\Theta) = K_{\rm s}(\Theta/\Theta_{\rm s})^{2b+3}$$

and

$$\psi(\Theta) = \psi_{\rm s}/(\Theta/\Theta_{\rm s})^b$$

where b is a curve-fitting parameter; $K_{\rm s}, \psi_{\rm s}$, and b depend on soil type.

The surface runoff model in the Simple Water Balance (SWB) model is selected to calculate the surface runoff R. The surface runoff R is defined as the excess of precipitation infiltrated not into the soil ($R = P_d - I_{\max}$), The maximum infiltration, $I_{\max}$, is formulated as

$$I_{\max} = P_d\frac{D_x[1-\exp(-kdt\delta_i)]}{P_d + D_x[1-\exp(-kdt\delta_i)]} ,$$

where, δ_i is the conversion of the current model time step, D_x is corrlated with the initial moisture condition that influence the infiltration process:

$$D_x = \sum_{i=1}^{4}\Delta Z_i(\Theta_{\rm s} - \Theta_i) ,$$

$P_d = (1-\sigma_f)P + D$ is the precipitation reaches the ground or the precipitation not intercepted by the canopy and

$$kdt = kdt_{\rm ref}\frac{K_{\rm s}}{K_{\rm ref}} .$$

where $kdt_{\rm ref} = 3.0$, $K_{\rm ref} = 2\times10^{-6}$ m s^{-1} (based on Chen and Dudhia, 2001), $K_{\rm s}$ is the saturated hydraulic conductivity, which depends on the soil texture.

The total evaporation E is the sum of (1) the direct evaporation from the top shallow soil layer $E_{\rm dir}$; (2) evaporation of precipitation intercepted by the canopy $E_{\rm c}$; and (3) transpiration via canopy and roots $E_{\rm t}$. That is, $E = E_{\rm dir} + E_{\rm c} + E_{\rm t}$.

A simple linear method was adapted for computing the direct evaporation from the ground surface:

$$E_{\rm dir} = (1-\sigma_{\rm f})\beta E_{\rm p}\ ,\ \ \beta = \frac{\Theta_1 - \Theta_{\rm w}}{\Theta_{\rm ref} - \Theta_{\rm w}}\ ,$$

where $E_{\rm p}$ is the potential evaporation, which is calculated by a Penman-based energy balance approach that includes a stability-dependent aerodynamic resistance, $\Theta_{\rm ref}$, and $\Theta_{\rm w}$ are the field capacity and wilting point, and $\sigma_{\rm f}$ is the green vegetation fraction, which is a critical for the partitioning of total evaporation between the bare soil direct evaporation and the canopy transpiration.

The wet canopy evaporation is determined by

$$E_{\rm c} = \sigma_{\rm f} E_{\rm p}\left(\frac{W_{\rm c}}{S}\right)^n\ ,$$

where $W_{\rm c}$ is the intercepted canopy water content, and S is the maximum canopy capacity. The budget for intercepted canopy water is

$$\frac{\partial W_{\rm c}}{\partial t} = \sigma_{\rm f} P - D - E_{\rm c}\ ,$$

where P is the input total precipitation. If $W_{\rm c}$ exceeds S, the excess precipitation or drip (D) reaches the ground.

The canopy evapotranspiration is determined by

$$E_{\rm t} = \sigma_{\rm f} E_{\rm p} B_{\rm c}\left[1 - \left(\frac{W_{\rm c}}{S}\right)^n\right]\ ,$$

where $B_{\rm c}$ is a function of canopy resistance and is formulated as

$$B_{\rm c} = \frac{1 + \dfrac{\Delta}{R_{\rm r}}}{1 + R_{\rm c}C_{\rm h} + \dfrac{\Delta}{R_{\rm r}}}\ ,$$

where $C_{\rm h}$ is the surface exchange coefficient for heat and moisture; Δ depends on the slope of the saturation specific humidity curve; $R_{\rm r}$ is a function of surface air temperature, surface pressure, and $C_{\rm h}$ and $R_{\rm c}$ is the canopy resistance.

3. Data and projects

Differences of the underlying surface physical characteristics between the oasis and the desert are obvious. The oasis grows very luxuriantly and the desertification happens hardly at all in the rainy season, but during the dry season the extreme drought climate and the arid environment can easily destroy the oasis because of its weak self-maintenance ability. Hence the summer in a dry year is selected as the simulation period.

First, a control experiment is designed and the simulation result is compared with the observations of the HEIFE field experiment. Then, a series of sensitivity experiments are planned to study the environmental influence caused by different oasis scales.

NCEP reanalyzed data are adapted as the large scale background fields. In order to compare with HEIFE observational data, August 1991 is selected. The initial condition is set as 2000 LST 1 August 1991. The vertical coordinate is terrain following. It is divided into 23 layers. The pressure at the top is 100 hPa. The central latitude and longitude in the control experiment is (38.93°N, 100.43°E). The horizontal grid distance is 1km. The grid numbers in the North-South direction and in the East-West direction are 37 and 41, respectively. The time step of iteration is 3 s and the simulation period is ten days.

In order to avoid the influence caused by a special weather condition and to analyze the self-development of the oasis, a series of sensitivity experiments is designed. The central latitude and longitude in the sensitivity experiments is (40°N, 101°E). The grid numbers are 45 in the East-West direction and 43 in the North-South direction. The horizontal resolution and the iterative time step are the same as the control experiment. $1^\circ \times 1^\circ$ NCEP reanalysis data are adapted also as the large scale background field. The ground surface fields and all the weather variable fields are assigned as flat. The surface fields such as the elevation field, the soil depth, the soil temperature field, and the soil moisture are set as the value of the center point where the desert is originally. The center point of the oasis is (23, 22). The land uses in the simulation region are set to be desert and there is an oasis of a set scale in the center of the desert. The surface albedo is 0.18 and 0.25 in oasis and desert, respectively. The roughness length is 15 cm and 1 cm, and the moisture available is 0.5 and 0.02, respectively. The soil moisture of the oasis is set to be 0.3 $\rm m^3\ m^{-3}$ higher than the other points. The specific humidity at the lowest σ layers is set to be 0.3 $\rm g\ kg^{-1}$ higher than the desert. The U, V wind field and air temperature field are set to be uniform at the beginning. The simulation period is 7 days. The simulation results of the different oases between 1 to 9 km, and a 0 km oasis, are analyzed to investigate the influences of different scale oases on the surroundings.

4. Analysis

First, the energy and mass exchange on the oasis ground surface is tested using MM5 in simulation to compare the simulation results with observations in

Table 1. The observed and simulated sensitive heat flux and latent heat flux.

Year	Month	Day	LST	Observed sensitive heat flux	Observed latent heat flux	Simulated sensitive heat flux	Simulated latent heat flux
1991	8	5	0800	14.3	27.1	35.10479	67.74413
1991	8	5	1400	162.7	245	190.0982	210.9259
1991	8	5	2000	1.5	–8.9	1.203065	6.576511
1991	8	6	0200	–0.1	–0.1	–4.492991	4.44954
1991	8	6	0800	18.8	38.2	23.68442	67.49877
1991	8	6	1400	116.4	221.3	187.174	213.1696
1991	8	6	2000	–0.5	–1.2	–2.514381	7.406713
1991	8	7	0200	–32.3	12.5	–4.778356	5.299225
1991	8	7	0800	–11.2	22.4	7.985923	58.72414
1991	8	7	1400	192.5	194.7	182.603	216.423
1991	8	7	2000	–33.9	48.1	-9.99×10^{-2}	14.30607
1991	8	8	0200	–12	6	–3.025568	7.122737
1991	8	8	0800	–0.4	6.9	11.47821	53.9288
1991	8	8	1400	155	240.8	168.6441	212.4984
1991	8	8	2000	–1.8	4.5	4.302904	8.759494
1991	8	9	0200	0.8	–8.4	–6.215726	5.267215
1991	8	9	0800	10	35.7	–0.303651	57.16902
1991	8	9	1400	134.1	294.7	158.8369	228.1163
1991	8	9	2000	–49.1	44.5	–17.57495	31.3999

IOP of the HEIFE field experiment. Then, the critical scale of the oasis is studied.

4.1 *Comparison of the simulation and the observations*

Here, the observation data used are the records at Zhangye station in the HEIHE database. Since observations were not recorded on 1–4, 10 and 11 August, the comparison period is from 0800 LST 5 August to 2000 LST 9 August 1991. Table 1 lists the simulated results and the sensitive heat flux and the latent heat flux observed in the comparison period. The sensitive and latent heat fluxes in the table are results calculated by Hu and Qi with a combination method using the observed data (Hu and Qi, 1993). Figure 1 shows the comparison of the sensitive and latent heat fluxes during the same time.

4.1.1 *Comparison of the sensitive heat flux*

It can be seen from Figs. 1a and 1b that the simulation matches well with the observations at Zhangye station. The coefficient of correlation between the simulated ground sensitive heat flux and the observed sensitive heat flux is as high as r^2=0.94. It can be calculated from Table 1 that the average sensitive heat flux of observation is about 35 W m^{-2}, and the mean of the simulation results is about 49 W m^{-2}. The difference between them is only 14 W m^{-2}. This illustrates that the simulated sensitive heat flux could stand for the real conditions over Zhangye's oasis.

4.1.2 *Comparison of the latent heat flux*

From Figs. 1c and 1d, we can conclude that the simulated latent heat flux agrees better with that observed at Zhangye station than the surface sensitive heat flux. We can calculate from Table 1 also that the average of the observed latent heat flux is about 75 W m^{-2}, and the mean of the simulated results is about 78 W m^{-2}. The difference between them is only 3 W m^{-2}. This indicates that the simulation could stand for the real conditions over the Zhangye oasis in this period. The coefficient of correlation between the simulation and the observations is as high as r^2=0.936.

In a word, the simulations agree well with observations in this period at Zhangye station. These results prove that MM5 could be used to simulate the energy and water vapor exchange over the oasis in NWC arid regions.

4.2 *Influence of the different oasis scales on the atmospheric fields over oasis*

The oasis affects locally the atmospheric field forming firstly a thermal inner boundary layer in which the energy and the moisture are exchanged between oasis and desert. Then, the exchange of the large scope energy and water vapor are conducted between the ground surface and the atmosphere over oasis and desert in the arid regions. The degree of oasis influence on the boundary layer is related greatly with its scale.

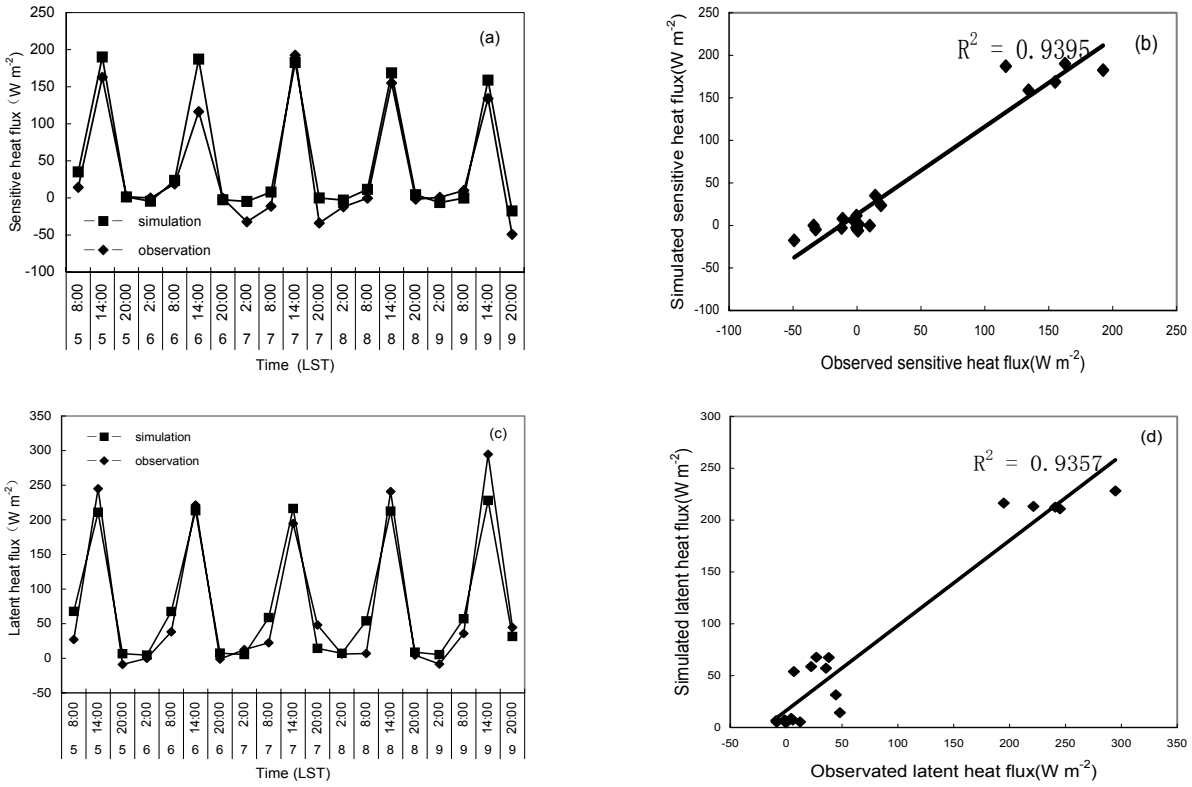

Fig. 1. Comparison of simulation and observation in IOP of HEIFE. (a) Comparison of simulated and observad sensitive heat flux; (b) correlation of simulated and observed sensitive heat flux; (c) comparison of simulated and observed latent heat flux; (d) correlation of simulated and observed latent heat flux.

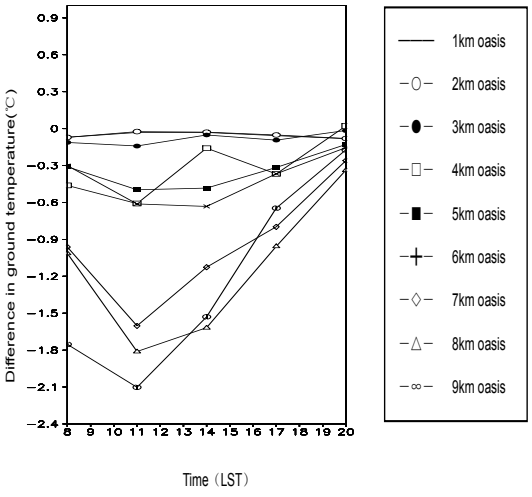

Fig. 2. Variation of difference in ground temperature between oasis and desert during 0800–2000 LST of the last day in the simulation period.

4.2.1 *Horizontal distribution of the temperature and specific humidity near the surface layer*

The great mass of net downward energy absorbed by the desert is used to heat the local soil and is transferred to the atmosphere through turbulence. While in the oasis, about 80% of the absorbed net energy is used for the plant transpiration. Just a little energy is used to heat the soil, and then it is transferred to the atmosphere. The vegetation transpiration transfers a large amount of moisture to the local atmosphere. It makes a cold source and a humid source of the oasis also in the surrounding drought environment. A cool and wet microclimate is formed that is favorable to plant growth (Su et al., 1987b).

Figure 2 shows the simulated ground temperature difference between the oasis center point and the surrounding desert from 0800 to 2000 LST on the last day of the simulation period. We can see that the ground temperature difference between the oasis center point and surrounding desert is mostly negative. Namely, the ground temperature of the oasis is lower than the surroundings. But the variation amplitude is different. The ground temperature difference between the oasis center point and the desert is very small in the daytime at the oasis scales of 1 km, 2 km, and 3 km; and it is nearly zero at 1400 LST. The temperature of the oasis is obviously lower than the desert, at oasis scales larger than 3 km. The variation of the ground temperature difference between the oasis center with

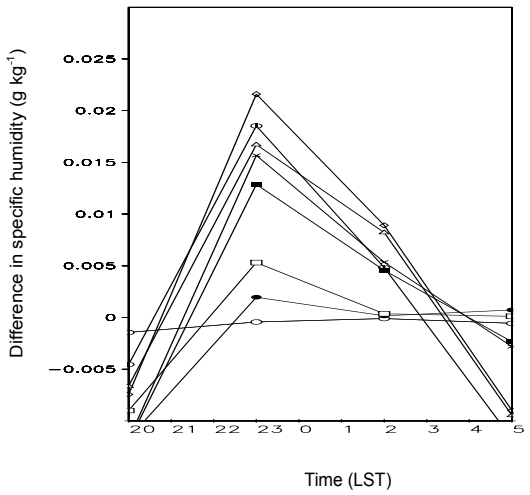

Fig. 3. Variation of specific humidity difference between oasis and desert at σ=0.995 during 2000–0500 LST of the last simulation day (Lines are the same as Fig. 2).

a 4 km scale and the surrounding desert is unstable. Sometimes, it is positive and sometimes negative. It is 0.1°C lower at the oasis center than in the desert surroundings at 1400 LST. At the same time, the ground temperature difference between the oasis with a 5–9-km scale and the surroundings is 0.5°C, 0.6°C, 1.1°C, 1.6°C, and 1.5°C, respectively. That is to say, the oasis is a cold source in contrast to the surrounding desert if the oasis scale is larger than 3 km (exclusive).

Figure 3 shows the simulated specific humidity difference at the lowest vertical level of the σ layer between the oasis and the surrounding desert from 2000 to 0500 LST of the last simulation day. We can conclude that the simulated specific humidity over the oasis is larger than the desert. But the variation amplitudes of different-scaled oases are not the same. The specific humidity of the lowest σ layer over the oasis is nearly the same as the desert for the oasis scales of 1km and 2 km; also the difference between them is nearly zero. But the humidity variations of other-scaled oases are not so. The specific humidity differences of the 4–9-km oases are positive. The difference becomes greater as the oasis scale becomes larger. The difference between the 3-km oasis and the surrounding desert is 2 mg kg^{-1}. The differences between the 4–9-km oases and their surroundings are 5 mg kg^{-1}, 13 mg kg^{-1}, 15 mg kg^{-1}, 16 mg kg^{-1}, 17 mg kg^{-1}, and 22 mg kg^{-1}, respectively. Namely, the oasis is a wet island in the surrounding desert if its scale is larger than 4 km.

We can conclude from the above analysis that the scale of 3 km is a key scale. The cold and wet environments take shape if the oasis scope is larger than this value. Even though an oasis of a scale of 4 km of a lower temperature and higher humidity than the surroundings sometimes this situation is unstable and could not last for a long time.

4.2.2 *Analysis of the mesoscale circulation*

As a result of the great difference in surface thermal characteristic between the oasis and the desert surroundings, there is a strong horizontal gradient in the horizontal temperature field at the intersection of the inner boundary layer of oasis and desert. The dry and hot air blocks are transferred to the adjacent oasis through advection and turbulent diffusion in the daytime. The sensitive heat flux is transferred downwards over the oasis. Likewise, the water vapor is led into the near desert margins from the oasis. All these form the integral image of the oasis-desert interaction. So the oasis-desert local thermal circulation is induced by the underlying horizontal thermal difference.

Figure 4 shows the simulated horizontal velocity field of the oases with 1 km and 9 km scales at the lowest vertical layer. Figure 4a gives the horizontal wind vector at 1400 LST in the daytime and Fig. 4b gives the one at 0200 LST in the night of the 9-km oasis. Figure 4c gives the horizontal wind field at 1400 LST and Fig. 4d gives the one at 0200 LST of the 1-km oasis. Clearly, the influence on local horizontal wind over the 1-km oasis is too weak to be shown in the circulation. But the influence on the u, v velocity over the 9-km oasis cover is strong. In the daytime, the horizontal wind field (u, v) over the 9-km oasis near the surface is divergent due to the obvious cooler surface temperature than the surroundings, and it is convergent at night. But for the 1-km oasis, the horizontal wind field background near the surface is not affected much in the daytime and at night, in spite of the oasis existence.

It is well known that if the horizontal velocity flow at the lower layer is convergent, the vertical wind will be upward, and it is downward when the lower layer wind flow is divergent. So let us focus on the vertical wind over the oasis center and the desert located downstream of the oasis.

Figure 5 is the simulated vertical wind over the oasis and its surrounding desert at the lowest vertical layer from 0800 to 2000 LST on the last day of the simulation period. We can see that the vertical wind speed is positive over the desert adjacent to the oasis. That is to say, the vertical air over the desert moves upward. The turbulence diffusion is very strong here. There are few differences among the sensitivity experiments. But this is not so over the oasis. Obviously, vertical wind speeds over the 1–3-km oases are mostly positive. Local air parcels move upwards. The turbulence over such oases is strong also. The cold and wet air is soon transferred into the arid surroundings by the turbulence exchange in the inner boundary layer.

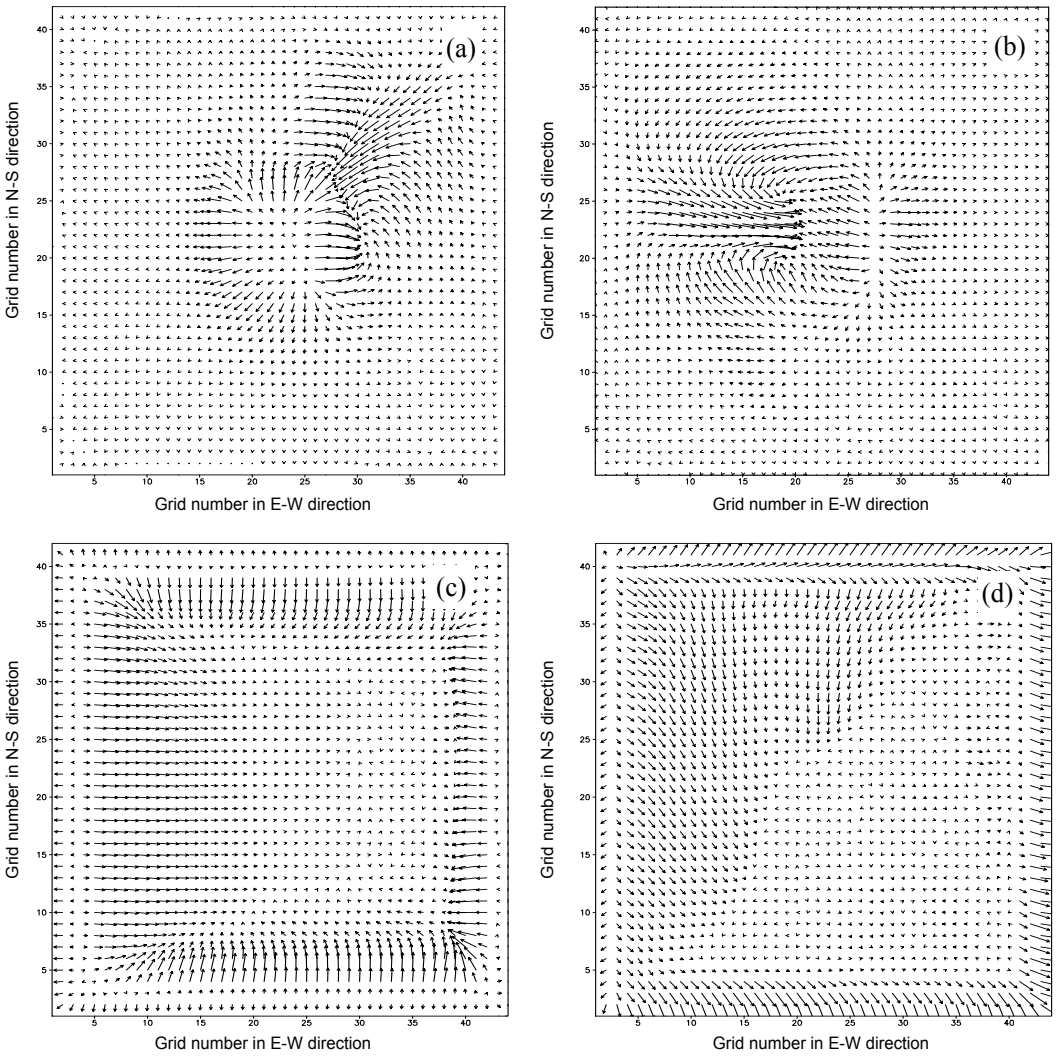

Fig. 4. Simulated u, v velocity vector at σ=0.995 of 1 km (c, d) and 9 km oasis (a, b) in the daytime (a, c) and at night (b, d).

The dry and hot air parcels over the desert are transported into the oasis soon from its lateral boundery because of the mass conservation principle. The cool and humid microclimate over the oasis is destroyed. So, the mechanics of maintaining and developing a stable and conservative oasis is destroyed. Such an oasis will not survive for a long time, even though it is in development. If the scale of the oasis reaches 4 km, the vertical movement is not steady. It is upwards mostly and downwards sometimes. This construction is also not favorable for oasis maintenance. When the oasis scale is larger than 4 km, the vertical wind movement of the cool and wet air over the oasis is mostly downward and it forms a local thermal circulation with the upward movement of hot and dry air over the adjacent desert. It is helpful to keep the environment ecosystem microclimate over the oasis to be moister and cooler than the surroundings, and this is favorable for oasis maintenance and development.

It can be concluded from the velocity field that an oasis whose scale is larger than 4 km easily forms the oasis-desert thermal local circulation. That is advantageous for the cool and moist construction over the oasis and contributes to maintain the stability of the oasis.

4.2.3 *Profile of the temperature and the humidity*

The oasis-desert circulation will affect the high layer atmospheric elemental field distribution. Let us see the profile of the temperature and the humidity.

Figure 6 is the simulated temperature profile over he oasis center at 1400 LST on the last day of the simulated period. We can see that the air temperature decreases progressively with the height if the oasis scale is smaller than 2 km. The moist air will be carried up-

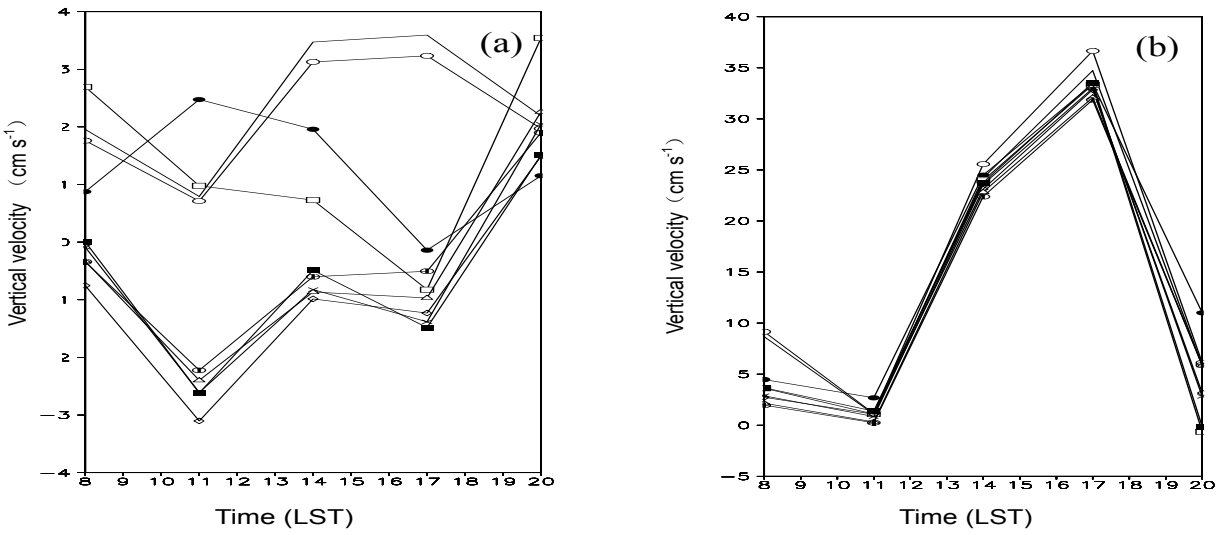

Fig. 5. Simulated variation of vertical velocity at σ=0.995 over oasis (a) and desert (b) at 1400 LST (Lines are the same as Fig. 2).

ward by the turbulence transportation, and then the dry and hot air will compensate from the surroundings. The hot and dry air will ruin the cool and moist microclimate over the oasis. The temperatures are constant and do not change with height where the height is lower than 200 m if the oasis scale is 2 km or 3 km. And, the air temperature decreases progressively with increasing height when the height is higher than 200 m. But if the oasis scale is larger than 4 km, there is a high temperature center at about 200 m to form an "inverse-temperature pattern". The "inverse-temperature pattern" forms a stable upper cover over the oasis. It enables the oasis to not be destroyed because the hot and dry air trespasses into it, to make the oasis a relatively isolated independent ecosystem. All these factors can keep the "cold island" existing steadily. Simultaneously, the "inverse-temperature pattern" restrains the development of the turbulence and the evapotranspiration. This is advantageous for crop growth inside the oasis.

Let us turn to the humidity profile over the desert downstream from the oasis. Figure 7 is the profile of specific humidity over the desert at 1400 LST on the last day of the simulated period. We can see that the specific humidity over the desert decreases gradually as height increases when the oasis scale is 1 km, 2 km, or 3 km. The maximum humidity is at the lowest vertical layer. When the scale of the oasis is larger than 4 km, the specific humidity does not decrease gradually with height. Under 200 m high, the humidity decreases gradually. But it increases with height from 200 m to 700 m, then decreases above 700 m. The maximum humidity is located at 700 m above the ground surface. So, an "inverse humidity pattern" is formed because the "inverse-temperature" layer restrains the evapotranspiration, and the water vapor cannot be transferred to higher levels. So, the water vapor is conveyed downstream into the desert just through the horizontal flow of the oasis-desert circulation near the surface.

A part of the water vapor reaching the desert could be reused by the sandy vegetation ecosystem in the transition zone of the oasis-desert. It is beneficial for sandy crop growth between the oasis and desert located downstream from the oasis, and it is favorable for extending the oasis. The water vapor recycle mechanism not only makes the oasis lose less moisture, but

Table 2. The horizontal scales of the fifteen oases in the Hexi region of Gansu Province.

No.	Oasis	Scale (km)
1	Wuwei	30
2	Mingqin	20
3	Gulang	23
4	Tianzhu	15
5	Jinchuan	17
6	Yongchang	8
7	Shandan	23
8	Mingle	17
9	Zhangye	19
10	Linze	17
11	Gaotai	23
12	Jiuquan	34
13	Jinta	42
14	Anxi	34
15	Dunhuang	46

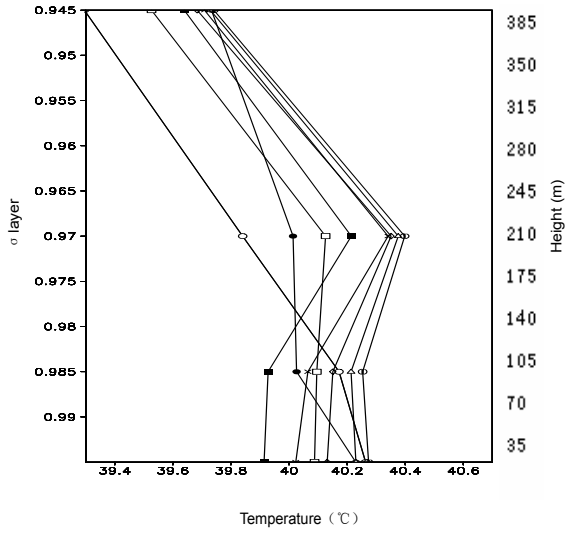

Fig. 6. Simulated air temperature profile over oasis center at 1400 LST (Lines are the same as Fig. 2).

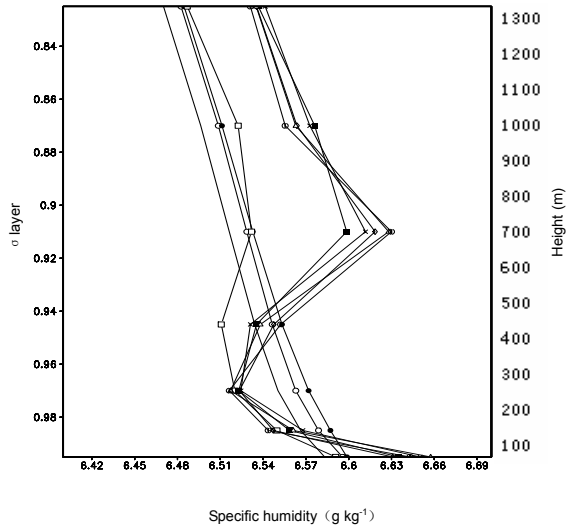

Fig. 7. Simulated specific humidity profile over desert located downstream of the oasis at 1400 LST (Lines are the same as Fig. 2).

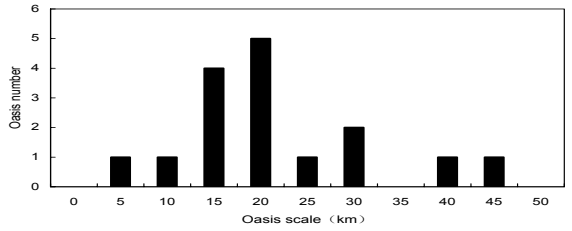

Fig. 8. Distribution histogram of oasis scales in the Hexi corridor, Gansu Province.

also the lost water of the oasis can be reutilized by the desert system adjacent to the oasis. All these factors can ensure that limited water resources in the oasis be used with higher efficiency, and this can overcome the water resources shortage of NWC. This is one of the main outcomes of oasis self-maintenance and development mechanisms (Zhang and Hu, 2001).

Considering the analysis of modelled horizontal and vertical temperature, humidity distribution, and mesoscale circulation, we can conclude that 4 km is a key scale for oasis self-maintenance and development.

4.2.4 *Statistics of oasis scale*

Table 2 lists the oasis horizontal scale statistically in the Hexi region (Zhang and Yu, 2001). Figure 8 is the histogram of the probability distribution. We can see from the table that the oasis scales are mainly concentrated within 8–46 km. Obviously, the number of oases smaller than 8 km is zero. This indicates that such an oasis cannot exist stably in nature. These statistical results also indirectly prove our above conclusion.

5. Conclusions and discussions

The above analysis supports shows the following conclusions:

(1) Using the NCAR nonhydrostatic mesoscale model MM5, the ground surface sensitive and latent heat flux are simulated at Zhangye City from 1 to 11 August 1991. Through a comparison with the HEIFE field experiment observations, it is verified that this model can be used to simulate the surface energy and water vapor cycles of the Zhangye oasis.

(2) The degree of influence of an oasis on the atmospheric fields depend on the oasis scale. The influence of an oasis on the atmospheric element fields are simulated and analyzed dynamically. The main conclusion is that the oasis-desert thermal circulation is formed only as the oasis scale is larger than 4 km. This oasis-desert thermal circulation will help to maintain the cool and moister microclimate over the oasis, even if the ground surface of the 3-km oasis is also cooler and moister than the surroundings. Just because of the local thermal circulation, the "inverse-temperature pattern" and "inverse-humidity pattern" are formed. The transpiration is restrained and this guarantees the stability and conservatism of the oasis. These are all advantageous not only for keeping the moisture over the oasis but also for the development of sandy crops on the fringe of the oasis, and provide the possibility for oasis maintenance and development. So, the 4 km scale is a critical scale of an oasis.

There are some insufficiencies in this research. For example, an ecological process scheme is not included in this model. The ecological effect therefore cannot be embodied. The critical scale of an oasis is a synthetic

index, which is geometric, thermal, dynamic, and so like the factors. More powerful proofs will be deduced if the ecological processes are involved and approached from more standpoints. Meanwhile, a long time simulation was not conducted because of computing time limits. Further quantitative description of oasis needs much further research on oasis in NWC arid and semiarid regions.

Acknowledgments. This study was supported by the National Natural Science Foundation of China under Grant Nos. 40233035, and 40075022, and the Innovative Project of the Chinese Academy Sciences (No.KZCX3-SW-329). The authors would like to thank Professors Hu Yinqiao and Zhang Qiang for their valuable suggestions. Professor Chen Fei of NCAR generously provided the user guide of OSULSM. Professors Wang Jieming and Ma Yaoming provided the observation data of HEIFE.

REFERENCES

Chen, F., and coauthors, 1996: Modeling of land-surface evaporation by four schemes and comparison with FIFE observations. *J. Geophys. Res.*, **101**, 7251–7268.

Chen Fei, and J. Dudhia, 2001: Coupling an advanced land surface-hydrology model with the penn State-NCAR MM5 modeling system. Part I: Model implementation and sensitivity. *Mon. Wea. Rev.*, **129**, 569–585.

Dudhia, Jimy, Dave Gill, Yong-Run Guo, Kevin Manning, Wei Wang, and Veronica Collin, 2001: PSU/NCAR mesoscale modeling system tutorial class notes and user's guide: MM5 modeling system version 3. 2001: 8.1–D.2.

Gao Yanhong, and Lu Shihua, 2001a: Numerical simulation of influence of different oasis distribution on regional climate. *Journal of Desert Research*, **21**(2), 108–115. (in Chinese)

Gao Yanhong, and Lu Shihua, 2001b: Numerical simulation of local climatic effect of heterogeneous underlying surface. *Plateau Meteorology*, **20**(4), 354–361. (in Chinese)

Grell, G. A., J. Dudhia, and D. R. Stauffer, 1995: A description of the fifth-generation penn State/NCAR mesoscale model (MM5). NCAR/TN-398+STR NCAR TECHNICAL NOTE, 37–90.

Hu Yinqiao, 1987: A result of numerical simulating of the strong cold island. *Plateau Meteorology*, **6**(1), 1–8. (in Chinese)

Hu Yinqiao, 1989: A special weather phenomenon in desert/Gobi—"the cold island effect". *Ziran Zazhi*, **12**(10), 773–777. (in Chinese)

Hu Yinqiao, and Wang Jiemin, 1989: The boundary layer physics in drought region and review about research of boundary layer physics in our institute. *Plateau Meteorology*, **8**(2), 133–138. (in Chinese)

Hu Yinqiao, and Qi Yuejin, 1993: The combinatory method for determination of the turbulent fluxes and universal functions in the surface layer. *Acta Meteorologica Sinica*, **7**(10), 101–109.

Hu Yinqiao, Gao Youxi, Wang Jiemin, Ji Guoliang, Shen Zhibao, Cheng Linsheng, Cheng Jiayi, and Li Shouqian, 1994: Some achievements in scientific research during HEIFE. *Plateau Meteorology*, **13** (3), 225–236. (in Chinese)

Jacquemin, B., and J. Noilhan, 1990: Sensitivity study and validation of a land surface parameterization using the HAPEX-MOBILHY data set. *Bound.-Layer Meteor.*, **52**, 93–134.

Ji Jinjun, and Miao Manqian. 1994: Numerical experiments of influence of heterogeneous vegetation distribution on the states of surface and atmospheric boundary layer. *Scientia Atmospherica Sinica*, **18**(3), 293–302. (in Chinese)

Mahrt, L., and H. L. Pan, 1984: A two-layer model of soil hydrology. *Bound.-Layer Meteor.*, **29**, 1–20.

Mahrt, L., and M. Ek, 1984: The influence of atmospheric stability on potential evaporation. *J. Climate Appl. Meteor*, **23**, 222–234.

Niu Guoyue, Hong Zhongxiang, and Sun Shufen, 1997: Numerical simulation on mesoscale fluxes generated by desert and oasis heterogeneous distribution. *Scientia Atmospherica Sinica*, **21**(4), 385–395. (in Chinese)

Noilhan, J., and S. Planton, 1989: A simple parameterization of land surface processes for meteorological models. *Mon. Wea. Rev.*, **117**, 536–549.

Pan, H. L., and L. Mahrt, 1987: Interaction between soil hydrology and boundary-layer development. *Bound.-Layer Meteor.*, **38**, 185–202.

Su Congxian, and Hu Yinqiao, 1988: Structure of the planetary boundary layer over oasis cold island. *Acta Meteorologica Sinica*, **2**(4), 527–534.

Su Congxian, Hu Yinqiao, Jiang Hao, Zhang Yongfeng, and Wei Guoan, 1987a: The observational research of the thermal flux and evapotranspiration in Hexi region. *Plateau Meteorology*, **6**(3), 217–224. (in Chinese)

Su Congxian, Hu Yinqiao, Zhang Yongfeng, and Wei Guoan, 1987b: Microclimate characteristics and "cold island effect" over the oasis in the Hexi region. *Chinese Journal of Atmospheric Sciences*, **11**(4), 443–451.

Xue Jukui, and Hu Yinqiao, 2001: Numerical simulation of oasis-desert interaction. *Progress in Natural Science*, **11**(9), 675–680.

Zhang Qiang, and Hu Yinqiao, 2001: Oasis effect in arid regions. *Ziran Zazhi*, **23**(4), 234–236. (in Chinese)

Zhang Qiang, and Yu Xuequan, 2001: Numerical simulation of oasis-induced mesoscale atmospheric flow and its sensitivity test of key factors. *Plateau Meteorology*, **20**(1), 58–65. (in Chinese)

Zhang Zhikun, and Sang Jianguo, 2000: A numerical simulation of mesoscale fluxes over an inhomogeneous underlying surface. *Chinese J. Atmos. Sci.*, **24**(5), 694–702. (in Chinese)